

# EFFECT OF DEPOSITION TIME AND MICROSTRUCTURE ON TRANSITION METAL MOLYBDENUM CHALCOGENIDES FOR PHOTOVOLTAIC APPLICATIONS

T.J.S. Anand<sup>1</sup>, S. Shariza<sup>2</sup>, S.I. Abd Razak<sup>3</sup> and C. Vedhi<sup>4</sup>

<sup>1</sup>Faculty of Mechanical and Manufacturing Engineering Technology,  
Universiti Teknikal Malaysia Melaka, Hang Tuah Jaya,  
76100 Durian Tunggal, Melaka, Malaysia.

<sup>2</sup>Faculty of Manufacturing Engineering,  
Universiti Teknikal Malaysia Melaka, Hang Tuah Jaya, 76100 Durian  
Tunggal, Melaka, Malaysia.

<sup>3</sup>Faculty of Biosciences & Medical Engineering,  
Universiti Teknologi Malaysia, Skudai, 81310  
Johor Bahru, Johor, Malaysia.

<sup>4</sup>Department of Chemistry,  
V.O. Chidambaram College, Tuticorin, 628 008,  
Tamilnadu, India.

Corresponding Author's Email: [1anand@utem.edu.my](mailto:1anand@utem.edu.my)

**Article History:** Received 25 October 2019; Revised 17 March 2020;  
Accepted 22 October 2020

**ABSTRACT:** This paper highlights into the synthesis of semiconductor materials, specifically transition metal chalcogenide thin films and the characterization of the films to evaluate the suitability for application as a photoelectrochemical (PEC) / solar cell. Electrodeposition technique is used that aims to design a safe, cost-efficient and relatively simple method for synthesis of the transition metal chalcogenide thin film for potential applications as PEC / solar cell manufacturing industry. Transition Metal chalcogenide ( $\text{MoX}_2$ ) thin films were successfully electrodeposited on conductive glass substrates and metal substrates in which the deposition time for the thin films were set up to 30 minutes with an interval time of 5 minutes. The thin films were characterized for their compositional and morphological characteristics by energy dispersive X-ray (EDX) analysis and scanning electron microscope (SEM) respectively. Addition of selenium element increases the orientation of crystals in the films are formed. The suitability of the thin films for photoelectrochemical (PEC) / solar cell applications, optical

and semiconducting parameters were analyzed. Films revealed it is of n-type nature with the Energy gap lying between 1.12 – 1.22 eV for the deposited films.

**KEYWORDS:** *Transition Metal Chalcogenides; Electrodeposition; Photoelectrochemical Cell*

## 1.0 INTRODUCTION

The current global energy crisis makes the researchers to focus their research on developing new renewable energy sources. Among various types of renewable energy sources, solar energy is promising owing to its environmental benignity, universality, high capacity and inexhaustibility [1]. With the depletion and cost escalation of conventional energy sources, much focus of research in this area has shifted to non-conventional energy sources.

Capturing solar energy through photovoltaic panels, in order to produce electricity is considered one of the most promising markets in the field of renewable energy [2]. The harnessing of one of the most abundant inexhaustible source of energy [3], namely solar energy for electrical energy conversion, still leaves much to be achieved. New materials are identified and efforts have been made by utilizing them for solar energy conversion. The main factor in fabricating these materials is the competitiveness of production cost and this particular factor can be greatly accomplished by producing the materials in thin film form [4].

Among the transition metal chalcogenide (TMC) materials of great interest are those in thin film form. TMC thin films such as CdZnS [5], BiSe [6], WSSe [7], NiSe [8], and CuSe [9] have been looked into by researchers for solar cell and photoelectrochemical (PEC) applications. Reports on the characterization of these materials have published that they have the ability to perform well as a PEC and solar cell materials.

Due to the factors above, the motivation to synthesis and study the transition metal chalcogenide thin films synthesized via electrodeposition technique for photoelectrochemical (PEC) / solar cell applications have been triggered in this research. However, far too little attention has been paid to electrodeposited ternary transition metal chalcogenides. This paper investigates ternary molybdenum chalcogenide thin films and its characterization.

## 2.0 EXPERIMENTAL METHODS

### 2.1 Cyclic Voltammetry Measurements

Prior to the deposition process, an electrochemical technique known as cyclic voltammetry (CV) was carried out to understand the reduction and growth of  $\text{MoS}_x\text{Se}_{2-x}$  ( $0 \leq x \leq 2$ ) thin films. In the mechanistic study of redox systems, CV studies is perhaps the most efficient and adaptable electroanalytical technique [10]. The potential limit for transition metal chalcogenide compounds was found to be suitable in the range of  $-1.05\text{ V}$  to  $1.05\text{ V}$  throughout the CV measurements done. It is in this potential range, the reduction and oxidation of the electrochemical active ion species take place for film formation.

The cyclic voltammogram of the electrodes in ammoniacal  $\text{H}_2\text{MoO}_4 + \text{Na}_2\text{S}_2\text{O}_3 \cdot 5\text{H}_2\text{O} + \text{SeO}_2$  (AR Grade with 99.5 % of chemicals) solution for deposition of  $\text{MoSSe}$  films ( $x=1$ ) is shown in Figure 1. During the forward scan, the cathodic current onset was observed to rise at  $-0.450\text{ V}$  and increased steadily thereafter. This phenomenon denotes the reduction of the cations in the electrolyte to form a stable  $\text{MoSSe}$  compound. However, in this case, hydrogen evolution is identified to occur at minimal rate due to the low current rise in the cathodic region. During the reverse scan, oxidation in the anodic region confirmed the dissolution of molybdenum sulphoselenide compound starting at approximately  $0.70\text{ V}$ .

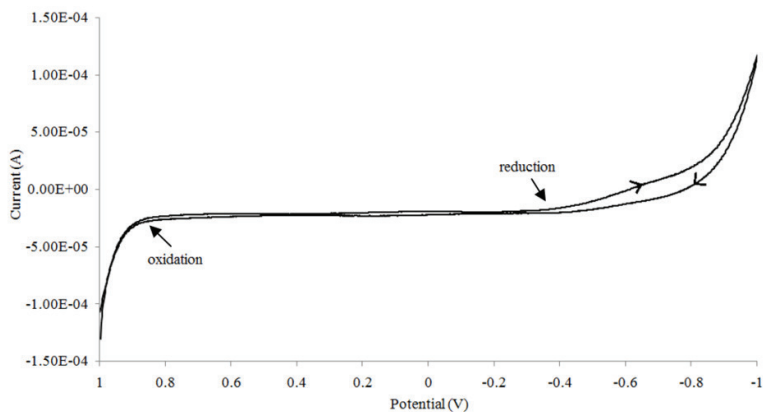


Figure 1: Cyclic voltammogram of the electrodes using glass substrates in ammoniacal  $\text{H}_2\text{MoO}_4 + \text{Na}_2\text{S}_2\text{O}_3 \cdot 5\text{H}_2\text{O} + \text{SeO}_2$  solution

The deposition of  $\text{MoS}_x\text{Se}_{2-x}$  ( $0 \leq x \leq 2$ ) thin films were carried out at the specific potential  $-1.05\text{ V}$  vs.  $\text{Ag}/\text{AgCl}$ ; on stainless steel substrates and ITO-coated glass substrates. Although theoretically the reduction of

the ions to form the films can occur at a less negative potential, the films were found to deposit on the substrates better at -1.0V. This was also observed for CV measurements using stainless steel substrates. The deposition time was set at 10 to 30 minutes with interval time 5 minutes while deposition temperature was controlled at  $40 \pm 1$  °C for  $\text{MoS}_x\text{Se}_{2-x}$  ( $x=0, 1$  and  $2$ ) thin films.

## 2.2 Electrodeposition of $\text{MoS}_x\text{Se}_{2-x}$ ( $0 \leq x \leq 2$ ) Thin Films

The CV analysis and electrodeposition of the film followed a system setup with three-electrodes. The setup and the schematic diagram of the system are shown in Figure 2. The electrolysis cell consisted of (i) reference electrode (RE): Ag/AgCl saturated calomel electrode (SCE) (ii) working electrode (WE): ITO-coated glass slide prepared as substrate or stainless steel foil as substrate; and (iii) counter electrode (CE): graphite. The two types of substrates (Metal and ITO glass slides) used to get stoichiometry results and nature of characterization studies. XRD prefers to be metal substrate to obtain crystalline results whereas optical studies prefer transparent glass slide as substrates.

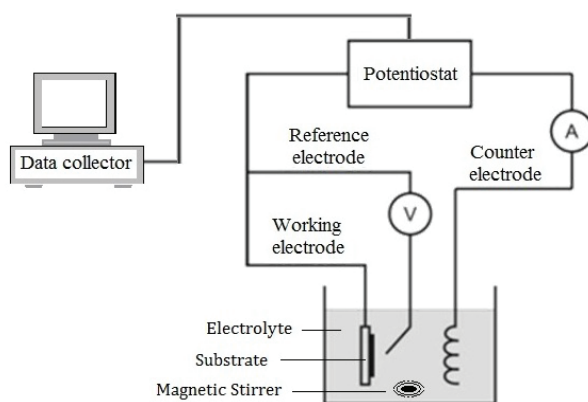


Figure 2: Schematic diagram of three-electrode cell system

The potential of the working electrode is measured by the SCE. To ensure the exact deposition potential is used the surface of the solution orifice will be monitored, it is placed very closely to the working electrode. Careful placement of the electrodes also ensures minimum effect of the internal resistance of the cell. Also, as a precaution method, the counter and working electrodes are adjusted to be barely 1 cm to each other. Simultaneously, to make certain that the cations will be attracted and deposited to the substrate surface; the two surfaces facing each other were kept parallel. The electrodes spacing should be

cautiously maintained to obtain the stoichiometric results. The thin films were characterized for their compositional and morphological characteristics by energy dispersive X-ray (EDX) analysis and scanning electron microscope (SEM) respectively. The suitability of the thin films for photoelectrochemical (PEC) / solar cell applications, optical and semiconducting parameters were analyzed.

### **3.0 RESULTS AND DISCUSSION**

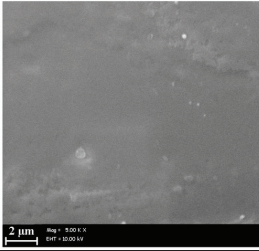
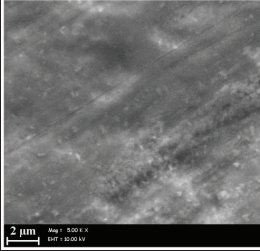
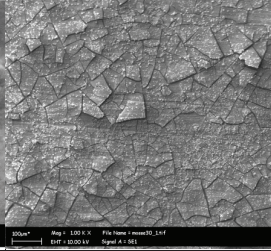
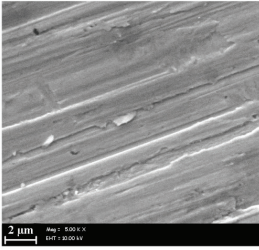
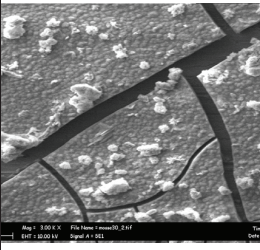
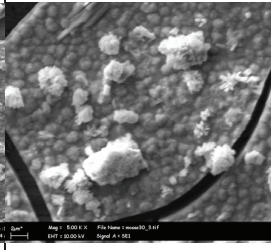
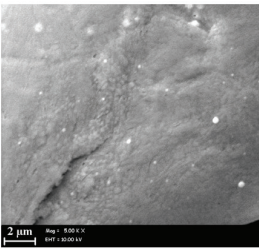
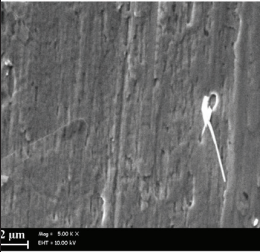
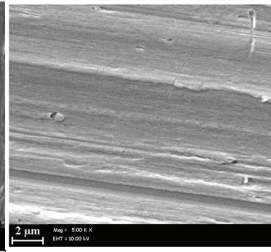
#### **3.1 Surface Morphology Studies of Thin Films**

The microstructural studies of the  $\text{MoS}_x\text{Se}_{2-x}$  ( $0 \leq x \leq 2$ ) thin films on stainless steel substrates were carried out by scanning electron microscope (SEM). SEM micrograph of the films at 30 minutes' deposition time are summarized in Fig 4 for both binary and ternary films at different magnification. Initially, the growth of the films was observed to be homogeneous and uniform. However, this is observed only in films of shorter deposition time (such as deposition time of 15 minutes).

The cracking of the films into segments (flakes); although still adhering to the substrate was observed at longer deposition times. Similar observation has been reported in films of thickness above 0.2  $\mu\text{m}$  as they are prone to cracking [11]. Hydrous films are well known to be at risk of drying shrinkage [12]. The grains of the materials keeps on growing with time; and upon reaching the maximum grain stress point, the films break and form flake-like structures. The highly conductive substrate continues to act as a growth plane for the films, which only comes to a saturated level at 30 minutes deposition time.

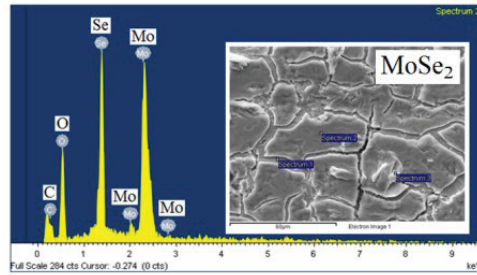
Apart from that, in ternary compound  $\text{MoSSe}$  thin films, the structure of the films seems to be inhomogeneous. Unsymmetrical crystallites are observed on the structure. The precipitation and separation of sulphide and selenide phases in ternary compounds causes unsymmetrical crystallites to form. This separation of phases in a ternary transition metal chalcogenide compound is also observed in the report by [13]. Another observation made is that films with higher selenium content have better surface morphology. As seen in Table 1, films of  $\text{MoSe}_2$  have smoother surface. While in  $\text{MoSSe}$  and  $\text{MoS}_2$  films, there are presences of crystallites observed especially in thicker films. Upon addition of selenium, better orientation of crystals in the films are formed.

Table 1: SEM micrographs of Molybdenum chalcogenide thin films deposited at 30 minutes

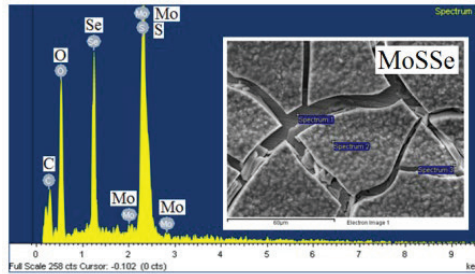
Deposition time 30 minutes	Magnification 1000x	Magnification 3000x	Magnification 5000x
For x = 0 , MoSe <sub>2</sub> thin film			
For x = 1 , MoSSe thin film			
For x = 2 , MoS <sub>2</sub> thin film			

### 3.2 Compositional Analysis of MoS<sub>x</sub>Se<sub>2-x</sub> (0 ≤ x ≤ 2) Thin Films

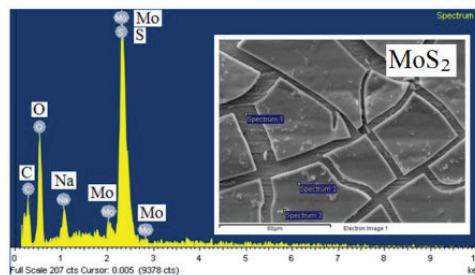
The quantitative analysis of these films deposited on metal (SS) substrates were carried out by using the EDX technique in nitrogen atmosphere to study the presence of molybdenum, sulphur and selenium elements in the stoichiometry of the films. Figure 3 shows the typical EDX patterns for these films deposited at 30 minutes.



(a)



(b)



(c)

Figure 3: Typical EDX patterns for (a) MoSe<sub>2</sub>, (b) MoSSe and (c) MoS<sub>2</sub> thin films deposited at 30 minutes

It is noticed that all spectra for the EDX of MoS<sub>x</sub>Se<sub>2-x</sub> ( $0 \leq x \leq 2$ ) thin films contained C and O elements. The EDX instrument is well known for detection of elements with low atomic number that are ubiquitous in our environment; such as oxygen and carbon [14]. Furthermore, in chemically deposited films, inclusion of oxygen is found to be unavoidable due to the aqueous nature of the electrolyte.

### 3.3 Optical Properties of MoS<sub>x</sub>Se<sub>2-x</sub> ( $0 \leq x \leq 2$ ) Films

The UV-Visible ray transmittance spectrum is capable of providing bandgap energy of these films through analysis of the Tauc plot. A distinct linear region in the plot denotes the onset of absorption of the

MoSe<sub>2</sub>, MoSSe and MoS<sub>2</sub> thin films and is shown in Figure 4. Hence, extrapolating this linear region to the x-axis stipulates the energy band gap of the material.

From the analysis, the bandgap of ternary MoSSe films are found to be transitional between those of binary MoS<sub>2</sub> and MoSe<sub>2</sub>. This can be implicit due to the stoichiometric nature of the films, where the amount of sulphur and selenide composition in MoSSe is in between the other two types of films. As observed, as the deposition time of the film increases, reciprocal to that the optical bandgap energy of all these films decreases. This correlates to film thickness, whereby a longer deposition time produces films with greater thickness. This trend is in agreement with Dheepa et al. [15] in a report on a transition metal sulphide compound. Tabulation of the film results for the bandgap energy with respect to its film thickness is presented in Table 2.

Table 2: Thickness of the films vs Bandgap energy values of MoS<sub>x</sub>Se<sub>2-x</sub> (0 ≤ x ≤ 2) thin films

Deposition Time (mins)	MoSe <sub>2</sub>		MoSSe		MoS <sub>2</sub>	
	Film Thickness (µm)	Energy Bandgap (eV)	Film Thickness (µm)	Energy Bandgap (eV)	Film Thickness (µm)	Energy Bandgap (eV)
30	1.162	1.12	1.158	1.44	1.157	1.64
25	1.107	1.15	1.067	1.50	1.093	1.67
20	1.027	1.17	0.992	1.54	0.955	1.70
15	0.945	1.20	0.914	1.61	0.862	1.72
10	0.888	1.22	0.842	1.66	0.803	1.74

When the deposition conditions such as solution concentration and temperature of the film are constant, the value of the band gap was observed to change with increasing film thickness. The possible reasons for this trend can be due to any of the following: (i) quantum size effect, (ii) changing barrier height because of variation in grain size in the polycrystalline film, or (iii) largeness of the dislocation [16]. The time-dependent parameters that affect the band gap are most likely due to self-oxidation of the film and reorganization of its crystal microstructure. It is hypothesized that as the deposition time increases, the voids of the films are filled, thus, denser films with smaller energy gaps are obtained [17].

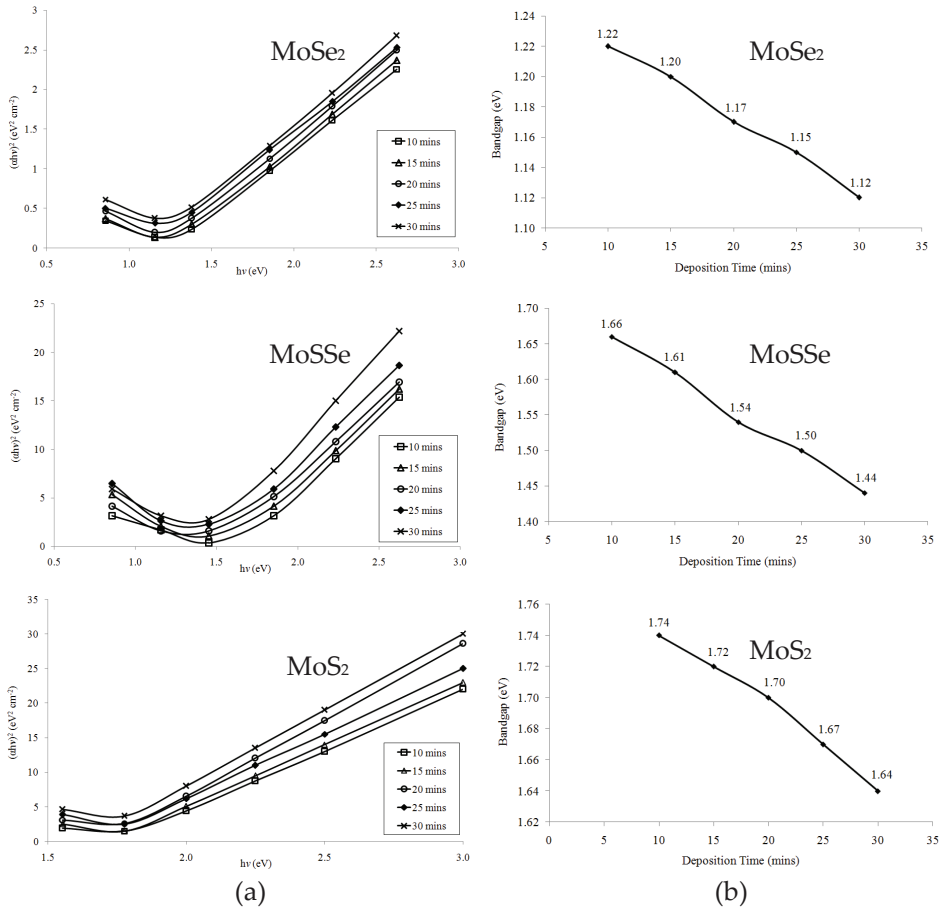


Figure 4: Variation of binary and ternary  $\text{MoS}_x\text{Se}_{2-x}$  ( $0 \leq x \leq 2$ ) with (a)  $(\alpha h\nu)^2$  vs.  $h\nu$  and (b) bandgap ( $E_g$ ) vs. deposition time of the  $\text{MoSe}_2$ ,  $\text{MoSSe}$  and  $\text{MoS}_2$  thin films, respectively

### 3.4 Semiconductor Parameters of $\text{MoSe}_2$ Films

The applied potential – capacitance behaviour data of  $\text{MoSe}_2$  thin films for the system  $\text{MoSe}_2 \mid 0.1 \text{ M (KI} + \text{I}_2 + \text{H}_2\text{SO}_4) \mid \text{graphite electrode}$  is carried out by plotting the applied potential versus inverse of the square of the capacitance to the films. Polyiodide electrolyte was used owing to unsuitability of polysulfide electrolyte for transition metal chalcogenide thin films. The Mott-Schottky plot for these films are shown in Figure 5. The intercept value on the voltage axis determines the flat band potential ( $V_{fb}$ ) value of the films. The obtained values of semiconductor parameters for the films are summarized in Table 3.

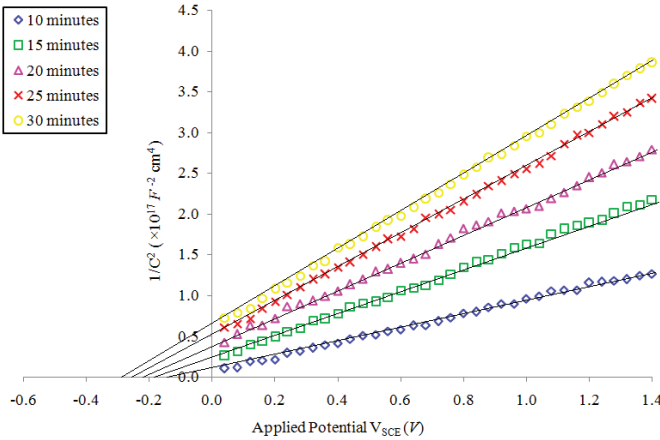


Figure 5: Mott-Schottky plot for MoSe<sub>2</sub> thin films at various deposition time

In order to conclude, the positive slope of the Mott-Schottky plots indicates that the MoS<sub>x</sub>Se<sub>2-x</sub> ( $0 \leq x \leq 2$ ) films are of n-type semiconductor. For all films, the value of  $V_{fb}$  was found to be reciprocal of thickness and decrease in thicker films. The value of  $V_{fb}$  is vital information as it establishes the limit of the cell photovoltage for solar cells [18]. The hypothesis that a narrow depletion width results in a smaller energy gap is fulfilled and proven in these results.

Table 3: Summary of the results obtained from the Mott-Schottky plots for MoSe<sub>2</sub> films

Semiconductor parameters	MoSe <sub>2</sub> thin film				
	30 minutes	25 minutes	20 minutes	15 minutes	10 minutes
Semiconductor type	n-type				
Band bending ( $V_b$ ) (V)	0.58	0.55	0.52	0.49	0.47
Energy gap ( $E_g$ ) (eV)	1.12	1.15	1.17	1.20	1.22
Flat band potential ( $V_{fb}$ ) (V)	-0.28	-0.25	-0.22	-0.19	-0.17
Dielectric constant ( $\epsilon$ )	33.5	34.1	37.3	39.0	44.1
Doping density ( $N$ ) $\times 10^{29}$ (m <sup>-3</sup> )	0.72	0.83	1.10	1.40	1.83
Depletion layer width ( $W$ ) (Å)	1.24	1.49	1.94	2.47	2.98
Density of states in Conduction Band ( $N_c$ ) $\times 10^{13}$ (m <sup>-3</sup> )	4.20	4.20	4.20	4.20	4.20

As the films become thicker, the dielectric constants are observed to decrease. The dielectric values determine the ability of materials to hold electrical charge for certain periods of time, and/or to keep great magnitudes of electric charge. Generally, when exposed to strong electric fields, materials with high dielectric constants fail more easily than those with low dielectric constants counterpart. Therefore, a decrease in the dielectric constant as the films become thicker is a desired property [18].

With the results of MoSe<sub>2</sub> films semiconductor parameters, an evaluation was done to assess the suitability of the MoS<sub>x</sub>Se<sub>2-x</sub> ( $0 \leq x \leq 2$ ) thin films as a photovoltaic cell material. All values measured proved that this molybdenum based binary and ternary thin films are competent as a PEC cell material [19].

#### 4.0 CONCLUSION

Molybdenum chalcogenide, MoS<sub>x</sub>Se<sub>2-x</sub> ( $0 \leq x \leq 2$ ) stoichiometric thin films were uniformly deposited via the electrodeposition technique. Generally, MoSSe ( $x=1$ ) thin films showed properties intermediate of the properties of MoSe<sub>2</sub> ( $x=0$ ) and MoS<sub>2</sub> ( $x=2$ ) thin films. The intermediate properties of the films are understood due to the stoichiometry and composition of the film for MoS<sub>x</sub>Se<sub>2-x</sub> from the end members of the series MoS<sub>x</sub>Se<sub>2-x</sub> (MoSe<sub>2</sub> and MoS<sub>2</sub>). The best film for all types was deposited at deposition potential of -1.0 V<sub>SCE</sub> and electrolyte temperature  $40 \pm 1$  °C. At deposition time 30 minutes, the thickness of the films becomes almost constant. An 'ion-by-ion' growth mechanism is evident due to the presence of induction period during film deposition. The surface morphology of the films determined via SEM showed that initially the growth of the films was observed to be uniform and well covered. EDX studies confirmed that mixed combinatorial films of molybdenum sulphoselenide, MoS<sub>x</sub>Se<sub>2-x</sub> ( $0 \leq x \leq 2$ ) have been formed. According to the results on the optical properties of the films, it can be concluded that the direct optical energy bandgap of all types of films fit into the range of a PEC / solar cell materials. Mott-Schottky analysis of MoS<sub>x</sub>Se<sub>2-x</sub> ( $0 \leq x \leq 2$ ) films revealed it is of n-type material. Semiconductor values measured to be in agreement with transition metal chalcogenides and prove that MoS<sub>x</sub>Se<sub>2-x</sub> ( $0 \leq x \leq 2$ ) thin films is competent as a PEC cell material.

## ACKNOWLEDGMENTS

The work presented in this manuscript was supported by the Ministry of Higher Education (MoHE), sponsored by KeTTHA/FRGS grant (Project No. FRGS/2011/FKP/TK02/1 F00120) and Universiti Teknikal Malaysia Melaka.

## REFERENCES

- [1] P. Zhang, B.Y. Guan, L. Yu and X.W. Lou, "Facile synthesis of multi-shelled ZnS-CdS cages with enhanced photoelectrochemical performance for solar energy conversion", *Chem*, vol. 4, no. 1, pp. 162-173, 2018.
- [2] P.G.V. Sampaio and M.O.A. González, "Photovoltaic solar energy: Conceptual framework", *Renewable and Sustainable Energy Reviews*, vol. 74, pp. 590-601, 2017.
- [3] G.K. Solanki, K.D. Patel, and R.B. Patel, "Synthesis, structural and photo electrochemical behaviour of SnSe<sub>0.5</sub>Te<sub>0.5</sub> single crystals", *Journal of Optoelectronics and Biomedical Materials*, vol. 2, no. 3, pp. 99-107, 2010.
- [4] T. Kobayashi, I. Yoshifumi, Y. Utsumi and H. Kanematsu, "Defects in aluminum thin films deposited on PET substrate and their formation mechanism", *Journal of Advanced Manufacturing Technology*, vol. 13, no. 1, pp. 71-82, 2019.
- [5] A.A.K. Bakly, B.F. Spencer and P. O'Brien, "The deposition of thin films of cadmium zinc sulfide Cd<sub>1-x</sub>Zn<sub>x</sub>S at 250 °C from spin-coated xanthato complexes: a potential route to window layers for photovoltaic cells", *Journal of Materials Science*, vol. 53, no. 6, pp. 4360-4370, 2018.
- [6] N.D. Desai, K.V. Khot, V.B. Ghanwat, S.D. Kharade and P.N. Bhosale, "Surfactant mediated synthesis of bismuth selenide thin films for photoelectrochemical solar cell applications", *Journal of Colloid and Interface Science*, vol. 514, pp. 250-261, 2018.
- [7] D.N. Gujarathi, G.K. Solanki, M.P. Deshpande and M.K. Agarwal, "PEC behaviour of mixed single crystals of tungsten sulphoselenide grown by a CVT technique", *Solar Energy Materials and Solar Cells*, vol. 90, no. 16, pp. 2630-2639, 2006.
- [8] T.J.S. Anand, R.K.M. Rajan, M.S. Kasim, S.M. Ho and R.T.R. Kumar, "Influence of deposition time on electrodeposited nickel selenide (NiSe<sub>2</sub>) thin films for solar/photoelectrochemical cells", *Journal of Advanced Manufacturing Technology*, vol. 12, no. 1(4), pp. 111-124, 2018.

- [9] F. Liu, J. Zhu, L. Hu, J. Yao, M.K. Nazeeruddin, M. Grätzel and S. Dai, "Low-temperature, solution-deposited metal chalcogenide films as highly efficient counter electrodes for sensitized solar cells", *Journal of Materials Chemistry A*, vol. 3, no. 12, pp. 6315-6323, 2015.
- [10] S. Ismail, F.I. Abu Bakar, B.A.W. Lee Yen, Z. Eshak and M. Rozana, "Preparation of cobalt decorated titanium dioxide nanotubes by electrodeposition", *Journal of Advanced Manufacturing Technology*, vol. 12, no. 1(4), pp. 99-110, 2018.
- [11] T.S. Joseph, M. Zaidan and S. Shariza, "Effect of additives on optical measurements of NiSe<sub>2</sub> thin films", *Procedia Engineering*, vol. 53, pp. 555-561, 2013.
- [12] M.A. Chavis, D.M. Smilgies, U.B. Wiesner and C.K. Ober, "Widely tunable morphologies in block copolymer thin films through solvent vapor annealing using mixtures of selective solvents", *Advanced Functional Materials*, vol. 25, no. 20, pp. 3057-3065, 2015.
- [13] K. Asokan, H.M. Tsai, C.W. Bao, J. W. Chiou, W.F. Pong, "Effect of Swift Heavy Ions in Ni-Al Nanocrystalline Films Studied by X-ray Absorption Spectroscopy", *Spectrochimica Acta – A*, vol. 70, no. 4, pp. 454-457, 2008.
- [14] W. Li, Y. Sun, W. Liu and L Zhou, "Fabrication of Cu(In, Ga)Se<sub>2</sub> thin films solar cell by selenization process with Se vapor" *Solar Energy*, vol. 80, no. 2, pp. 191-195, 2006.
- [15] J. Dheepa, R. Sathyamoorthy and A. Subbarayan, "Optical properties of thermally evaporated Bi<sub>2</sub>Te<sub>3</sub> thin films", *Journal of Crystal Growth*, vol. 274, no. 1-2, pp. 100-105, 2005.
- [16] E. Guneri, C. Ulutas, F. Kirmizigul, G. Altindemir, F. Gode, and C. Gumus, "Effect of deposition time on structural, electrical and optical properties of SnS thin films deposited by chemical bath deposition", *Applied Surface Science*, vol. 257, no. 4, pp. 1189-1195, 2010.
- [17] H. Metin and R. Esen, "Annealing studies on CBD grown CdS thin films", *Journal of Crystal Growth*, vol. 258, no. 1-2, pp. 141-148, 2003.
- [18] H.J. Park, J.H. Lee, B.U. Min, and S.J. Kim, "The effect of post annealing on physical properties of NiTe<sub>2</sub> thin film fabricated by magnetron sputtering", *Journal of Korean Institute of Metals and Materials*, vol. 58, no. 3, pp. 195-200, 2020.

- [19] C.K. Sumesh, "Towards efficient photon management in nanostructured solar cells: Role of 2D layered transition metal dichalcogenide semiconductors", *Solar Energy Materials and Solar Cells*, vol. 192, pp. 16-23, 2019.